Title	Towards Atomic Level Simulation of Electron Devices Including the Semiconductor-Oxide Interface
Author(s)	Markov, SN; Aradi, B; Yam, CY; Chen, G; Frauenheim, T
Citation	International Conference on Simulation of Semiconductor Processes and Devices (SISPAD), Yokohama, Japan, 9-11 September 2014. In International Conference on Simulation of Semiconductor Processes and Devices Proceedings, 2014, p. 65-68
Issued Date	2014
URL	http://hdl.handle.net/10722/201195
Rights	International Conference on Simulation of Semiconductor Processes and Devices Proceedings. Copyright © I E E E.

Towards Atomic Level Simulation of Electron Devices Including the Semiconductor-Oxide Interface

Stanislav Markov, ChiYung Yam, GuanHua Chen
Department of Chemistry
The University of Hong Kong
Hong Kong SAR, China
figaro@hku.hk

Bálint Aradi, Gabriele Penazzi, Thomas Frauenheim
Bremen Center for Computational Materials Science
University of Bremen
Bremen, Germany

Abstract—**We report a milestone in device modeling whereby a planar MOSFET with extremely thin silicon on insulator channel is simulated at the atomic level, including significant parts of the gate and buried oxides explicitly in the simulation domain, in *ab initio* fashion, i.e without material or geometrical parameters. We use the density-functional-based tight-binding formalism for constructing the device Hamiltonian, and non-equilibrium Green's functions formalism for calculating electron current. Simulations of Si/SiO_2 super-cells agree very well with experimentally observed band-structure phenomena in SiO_2-confined sub-6 nm thick Si films. Device simulations of ETSOI MOSFET with 3 nm channel length and sub-nm channel thickness also agree well with reported measurements of the transfer characteristics of a similar transistor.**

Keywords—atomistic modelling; density functional tight binding; MOSFET; silicon-on-insulator; silicon dioxide

I. INTRODUCTION

Atomic level modeling of transport phenomena in electron devices becomes increasingly relevant due to continuous miniaturization of technology and growing diversity of device architectures and materials. It is typically accomplished by coupling an atomistic device Hamiltonian to the non-equilibrium Green's functions (NEGF) formalism. Two popular choices to build atomistic Hamiltonian are density functional theory (DFT) and empirical tight binding (ETB) [1, 2]. The extreme complexity of the former, and the limited transferability of the latter across structural interfaces and amorphous materials have narrowed their scope of application to transport through hydrogen-passivated channels only. However, in ultra-thin films and narrow nanowires the band-structure, quantization, and interface scattering critically depend on the amount of confinement and on the intricacy of the semiconductor-oxide interface [3–5].

Here we report a milestone in device modeling, whereby a significant part of the gate-oxide and of the buried-oxide (BOX) of a MOSFET with a channel of extremely thin Si-on-insulator (ETSOI) are explicitly included in the drain current calculation at atomic level, for the first time.

II. METHODOLOGY

We employ the DFTB+ computer code, implementing the spin-polarized, self-consistent-charge density-functional-based tight binding (DFTB), extended by NEGF for transport [6–8]. The Hamiltonian and overlap matrix elements in DFTB are calculated *ab initio* from DFT with a linear combination of optimized atomic orbitals as a basis, and tabulated with respect to inter-atomic distance, thus accounting for interactions between an extended number of neighbors. Together with a self-consistent energy term due to second-order charge fluctuations, this makes DFTB efficient, yet accurate way to calculate electronic structure even for amorphous oxides and semiconductor-oxide interfaces. DFTB permits parametrization (2–3 parameters per chemical element) through the optimization of the atomic orbitals used as a basis. Tables of the Hamiltonian and overlap matrix elements versus distance are distributed through www.dftb.org. However, we find that these are not of sufficient accuracy for semiconductor device simulation, and in this work we re-optimize the parameters against well-known experimental band-structure data of Si.

Fig. 1(a) and (b) show the atomic structure of the interface models used in the study. We are interested in modeling planar ETSOI devices, and therefore compare the conventional model of H-terminated Si film with the α-quartz SiO_2/Si superlattice model from [3]. Based on the latter, we build the principle layer (PL) shown in Fig. 1(c), which is repeated in the transport
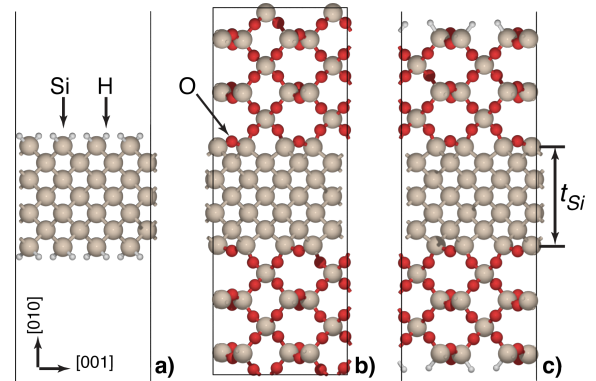

Fig. 1. Orthographic view along [100] direction of the atomic structure of the supercells (repeated 2x2x1) used in band-structure calculations of **(a)** H-, and **(b)** SiO_2-confined, 0.8nm thick Si film. H-termination of Si corresponds to the Si(001)1x1 symmetric dihydrate structure from [15]. The α-quartz SiO_2-Si supercell is from [3]. **(c)** Principle layer (PL) used in constructiing the atomic model of the ETSOI transistor, based on the supercell in (b), by splitting the oxide in top and bottom oxides of 1 nm and passivating them by H. Vacuum buffer of 4 nm is added in (a) and (c).
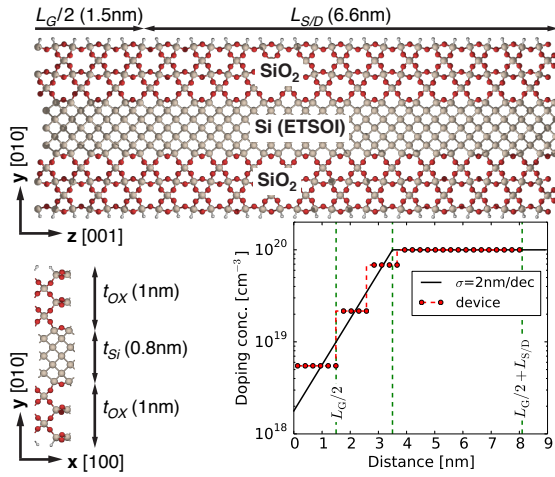
Fig. 2. Orthographic views of the *right-half* of the simulated device, viewed along [100] and [001] directions. Vacuum buffer extends the simulation domain to 7 nm in Y. Periodicity in X is imposed. Inset shows the n-type doping profile (right half only; see text for details).

direction [001], to create an ETSOI MOSFET shown in Fig. 2. The device has 3 nm gate length (L_G) and ~7 nm source/drain extensions ($L_{S/D}$), connected to semi-infinite leads of the same atomic structure as the PL. The atomic model of ~1700 atoms comprises 1 nm gated SiO_2, 0.8 nm Si channel, and the first 1 nm of a thick BOX. Transport is in [001] (Z), oxide confinement in [010] (Y) directions. Periodicity is imposed in [100] (X) direction, consistent with a very wide, planar device. Virtual crystal approximation is adopted for n-type doping [22], and no chemical impurity is introduced, eliminating device variability. Note however, that we do not recalculate the Hamiltonian matrix elements, and therefore do not capture the band-gap narrowing in the source/drain regions. Doping profile is depicted in the inset of Fig. 2. The step-like doping within 2 nm away from the gate edge is the effective density assigned to the Si atoms in the channel of each PL, corresponding to an exponentially decaying ion concentration at a rate of one decade per 2nm. The device is simulated by coupling the DFTB Hamiltonian to NEGF and Poisson electrostatics in a self-consistent loop within the DFTB+ computer code. Metal gate is represented by Dirichlet boundary condition, applied away from the SiO_2 structure, to ensure an effective oxide thickness (EOT) of 1.5 nm. Simulations are performed on a 4-core Dell Optiplex workstation.

III. Results and Discussion

First we demonstrate the applicability of DFTB to electronic structure in the context of bulk and interfacial Si and SiO_2. Fig. 3 shows very good agreement with experiment for the band-structure of bulk Si calculated in DFTB with our parameterisation for Si. Spin-orbit coupling is included. Notably, indirect band-gap is 1.129 eV with conduction band minimum at 0.81 of the Γ–X line (vs. experimental values of 1.12 eV and 0.85 [19]). Conduction and valence band effective masses are within 15% of experiment as reported in Fig. 3. The band-structure of bulk α-quartz SiO_2, calculated with DFTB is shown in Fig. 4. Atomic structure of the unit cell of α-quartz is from [11]. The error in the fundamental gap here is larger (~25%), but nevertheless a wide-gap insulator results. Recall

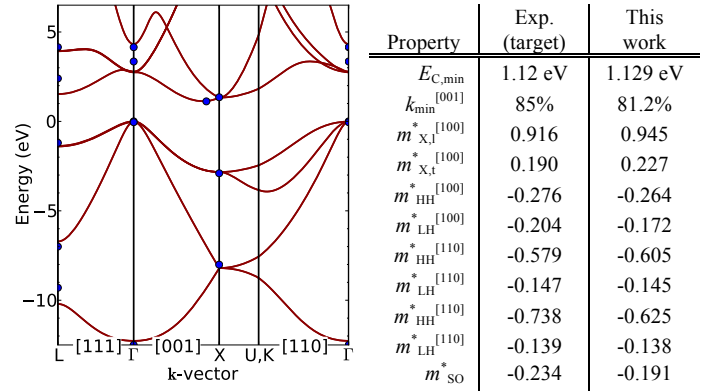| Property	Exp. (target)	This work
$E_{C,min}$	1.12 eV	1.129 eV
$k_{min}^{[001]}$	85%	81.2%
$m^*_{X,l}{}^{[100]}$	0.916	0.945
$m^*_{X,t}{}^{[100]}$	0.190	0.227
$m^*_{HH}{}^{[100]}$	-0.276	-0.264
$m^*_{LH}{}^{[100]}$	-0.204	-0.172
$m^*_{HH}{}^{[110]}$	-0.579	-0.605
$m^*_{LH}{}^{[110]}$	-0.147	-0.145
$m^*_{HH}{}^{[110]}$	-0.738	-0.625
$m^*_{LH}{}^{[110]}$	-0.139	-0.138
m^*_{SO}	-0.234	-0.191

Fig. 3. Band-structure of bulk Si calculated with DFTB (lines) using the parametrisation obtained in this work, showing very good agreement with target energies at points of high-symmetry (symbols). Si representation is $3s^2 3p^2 3d^0$. Effective masses also agree well with experiment [19].
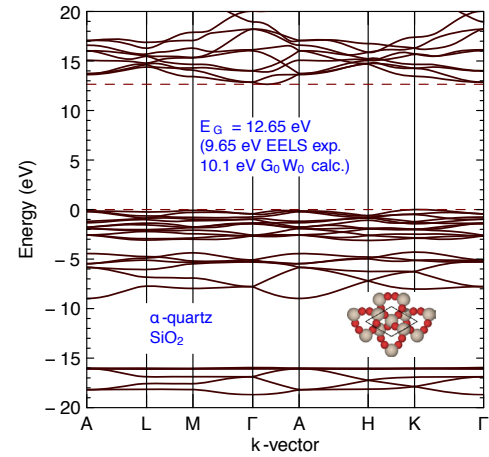

Fig. 4. Band-structure of bulk α-quartz SiO_2 calculated with DFTB using the parameters obtained in this work. Valence band is in good agreement with DFT and more accurate theories. Bandgap is larger (~25%) than experimentally known [11], due to a poorly expressed minimum near Γ.
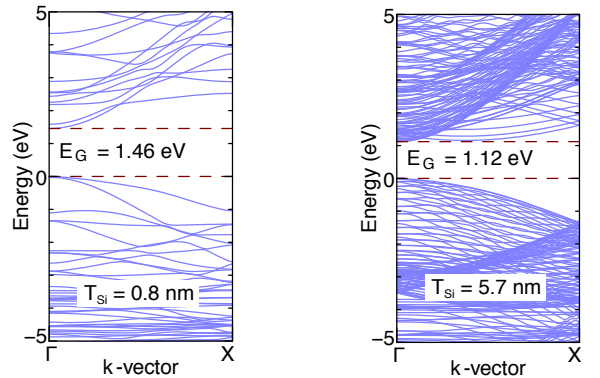

Fig. 5. Band-structure along the Γ–X line of the tetragonal Si/SiO2 supercell, for two different thicknesses of the Si film, calculated in DFTB. Top of the valence band is taken as a reference in both cases.

that conventional simulations with DFT in the local density or generalized gradient approximations underestimate the band-gap of Si and SiO_2 almost by a factor of two. We find that the error here is due to the poorly expressed conduction band-minimum at Γ and that the small disorder, as found in the
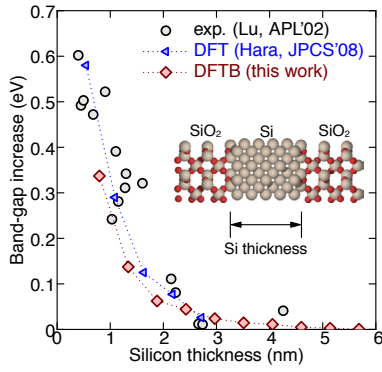
Fig. 6. Widening of Si band-gap with the decreasing thickness of SiO₂-confined Si film is accurately modeled by DFTB, as compared to experimental data from from [16] and DFT calculations from [13].
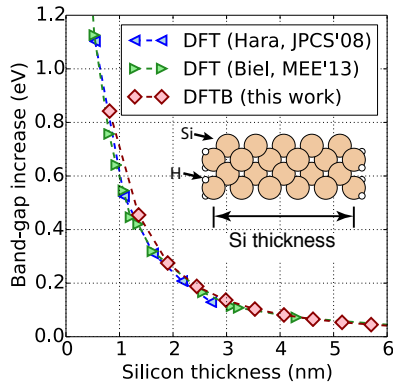

Fig. 7. Widening of Si band-gap with the decreasing thickness of hydrogen-confined Si film is accurately modeled by DFTB, as compared to DFT calculations from [13], and [14]. Note the two times larger magnitude of the effect, in comparison to the SiO₂-confined Si film of Fig. 6.

atomic model of the Si/SiO₂ interface, lowers the band-gap somewhat closer to experiment.

The Si/SiO₂ super-cell in Fig. 1(b) can be regarded as a unit cell of a tetragonal lattice. The Γ-X path of its first Brillion zone (BZ) is the same as the Γ-X path of the BZ of bulk Si (FCC lattice). The band-structure of the Si/SiO₂ super-cell along the Γ-X path, calculated within DFTB is shown in Fig. 5 for two different thicknesses of Si. It exhibits the well-known transition to direct band-gap in ultra-thin Si, as obtained from DFT calculations and experimentally suggested by the enhanced photo-luminance of such films [20, 21]. This phenomenon is concomitant with a widening of the band-gap of Si, as film-thickness decreases. In Fig. 6, we show a very good agreement between DFTB calculation and experiment for this band-gap widening. Results of Fig. 6 should be compared with those of Fig. 7, showing the same relation in the case of hydrogen-terminated Si film, *c.f.* Fig. 1(a). Note that H-termination leads to the same qualitative trend, but overestimates the magnitude of the effect by a factor of two, demonstrating the importance of including the oxide explicitly in the atomic model.

Fig. 8 and Fig. 9 show that DFTB describes well the gradual transition of the band-gap across the Si-SiO₂ interface, which is known to depend on extended-neighbor interactions of the sub-stoichiometric species at the interface [9].
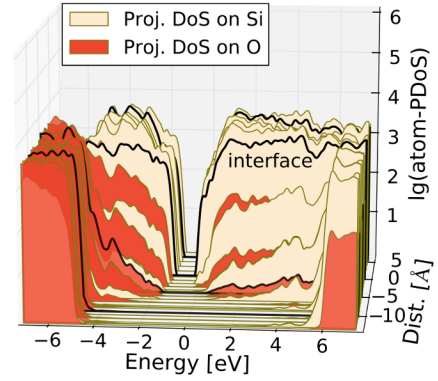

Fig. 8. On-atom projected density of states (pDOS) across the Si-SiO₂ interface, showing the gradual widening of the band-gap within the oxide.
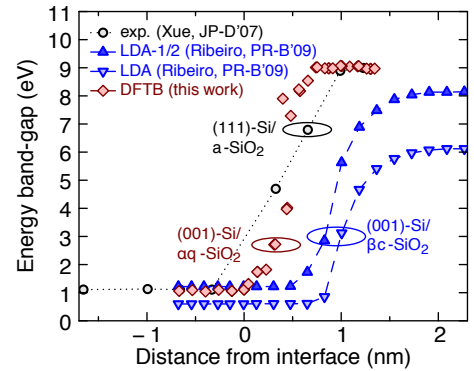

Fig. 9. Evolution of the band-gap across the Si-SiO₂ interface obtained from DFTB compares well to experiment [17] and DFT theory [18].

Next, we present simulations of drain current through the ETSOI device structure described in Fig. 2. Fig. 10(a) shows the electrostatic potential in the simulation domain, and the fluctuations in the potential are correlated to the atomic structure in Fig. 10(b). The transfer characteristics of the device at 50 mV and 300 mV drain bias are reported in Fig. 11, and a broad comparison is attempted against the V-groove junctionless MOSFET with 3nm gate length and sub-nm Si thickness from [10]. A detailed comparison is hard to attempt due to the following. The donor density in the channel and around the gate edges is not exactly known; neither the exact Si body thickness can be ascertained. We find that the doping concentration near the gate edges critically affects the sub-threshold characteristics of the device, due to source-to-drain tunneling. While the doping assumed in our study (see inset in Fig. 2) gives good agreement of the sub-threshold slope at 50 mV drain bias, the poor DIBL suggests lower concentration near the edge of the gate in the experiment. The more significant deviation of the simulations from experiment is in the on-current, however. Simulations largely overestimate the current at high gate bias due to the lack of impurity scattering in the source and drain. Some error may be expected due to the lack of surface roughness [5], but negligible effect of phonon scattering is expected at this gate length. While these aspects demand further improvement of the approach, they are not so important in the sub-threshold regime, where we note that without any parameter entering the device model, simulation results are already reasonably close to measurements.
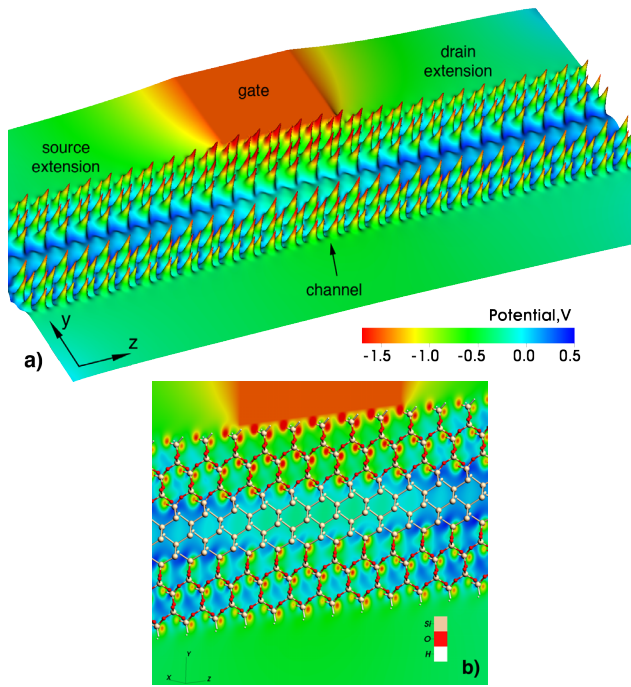
Fig. 10. Electrostatic potential in an YZ-plane of the device through the middle of the atomic structure in X direction. The elevated plot in a) shows the entire simulation domain, and large potential barriers in the oxide. The plot in b) shows augmented channel region with the atomic structure superposed and viewed off-[101] direction, correlating the large potential peaks with the oxygen atoms. $V_{GS} = 0$ V, $V_{DS} = 50$ mV.

IV. CONCLUSIONS

DFTB coupled to NEGF and self-consistent Poisson electrostatics constitute a promising approach for atomic level simulation of electron devices with extremely thin/narrow channel, in which the semiconductor-oxide interface plays a decisive role on the electrical characteristic and demands explicit modeling. Good agreement with measured transfer characteristics is obtained, but doping density and channel thickness are a degree of freedom. A major challenge of the approach is accounting for impurity scattering, without introducing chemical doping.

ACKNOWLEDGMENT

Fig. 11. Transfer characteristics of the simulated device compared to measurements of a V-groove MOSFET with $L_G = 3$nm and $T_{Si} < 1$nm from [10].

REFERENCES

[1] J. Maassen, M. Harb, V. Michaud-Rioux, Y. Zhu, and H. Guo, "Quantum transport modeling from first principles" *Proc. IEEE* vol. 101, pp. 518 – 530, 2013.

[2] G. Klimeck, S.S. Ahmed, B. Hansang, N. Kharche, S. Clark *et al,* "Atomistic simulation of realistically sized nanodevices using NEMO 3-D—Part I: models and benchmarks," *IEEE Trans. Elec. Dev.* Vol. 54, no. 9, pp. 2079 – 2089, 2007.

[3] S. Markov, P. V. Sushko, S. Roy, C. Fiegna, E. Sangiorgi, A. L. Shluger, and A. Asenov, "Si–SiO2 interface band-gap transition – effects on MOS inversion layer", *Phys. Stat. Sol.(a)* Vol. 205, No. 6, pp.1290-1295, 2008.

[4] D. Lizzit, D. Esseni, P. Palestri, L. Selmi, "Surface roughness limited mobility modeling in ultra-thin SOI and quantum well III-V MOSFETs." *Proc. IEDM,* p.120, 2013.
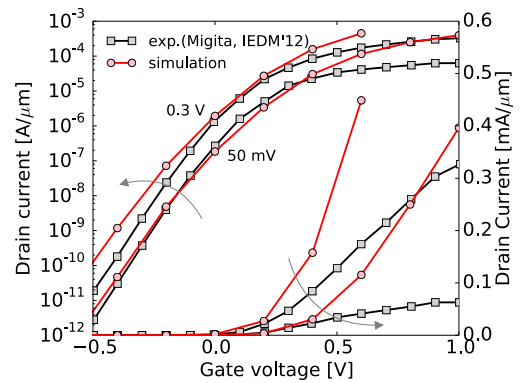
[5] N. Mori, G. Mil'nikov, H. Minari, Y. Kamakura, T. Zushi, *et al,* "Nano-device simulation from an atomistic view" , *Proc. IEDM,* p.114, 2013.

[6] T. Frauenheim, G. Seifert, M. Elstner, T. Niehaus, C. Köhler *et al*, "Atomistic simulations of complex materials: ground-state and excited-state properties," *J. Phys.: Cond. Matt*, Vol. 14 p.3015, 2002.

[7] A. Pecchia, G. Penazzi, L. Salvucci, and A. Di Carlo, "Non-equilibrium Green's functions in density functional tight binding: method and applications," *New J. Phys.*, Vol. 10, p.065022, 2008.

[8] B. Aradi, B. Hourahine, Th. Frauenheim, "DFTB+, a sparse matrix-based implementation of the DFTB method," *J. Phys. Chem. A*, Vol. 111(26), p. 5678, 2007 (code available online www.dftb-plus.info).

[9] J. Neaton, D.A. Muller, and, N.W. Ashcroft, "Electronic properties of the Si/SiO$_2$ interface from first principles," *Phys. Rev. Lett.,* Vol. 85, p.1298, 2000.

[10] S. Migita, Y. Morita, M. Masahara, and H. Ota, "Electrical Performances of Junctionless-FETs at the Scaling Limit (L_{CH} = 3 nm)," *Proc. IEDM* p.191, 2012.

[11] L. Garvie, P. Rez, J.R. Alvarez, P.R. Buseck, A.J. Craven, and R. Brydson, "Bonding in alpha-quartz SiO2: A review of the unoccupied states," *Am. Mineral.*, Vol. 85 p.732, 2000.

[12] E. Chang, M. Rohlfing, and S. G. Louie, "Excitons and optical properties of alpha-quartz," *Phys. Rev. Lett.*, Vol. 85 p.2613, 2000.

[13] T. Hara, Y Yamada, T Maegawa, and H Tsuchiya, "Atomistic study on electronic properties of nanoscale SOI channels," *J. Phys.: Conf. Ser.,* Vol. 109, p.012012, 2008.

[14] B. Biel, L. Donetti, A. Godoy, and F. Gámiz, "*Ab initio* validation of continuum models parametrizations for ultrascaled SOI interfaces," *Microelec. Eng.,* Vol. 109 p.286, 2013.

[15] J. Northrup, "Structure of Si(100) H: Dependence of the H chemical potential," *Phys. Rev. B*, Vol. 44, p.1419, 1991.

[16] Z. Lu and D. Grozea, "Crystalline Si/SiO2 quantum wells," *Appl. Phys. Lett.*, Vol. 80 (2002) p.255.

[17] K. Xue, H.P. Ho, and, J.B. Xu, "Local study of thickness-dependent electronic properties of ultrathin silicon oxide near SiO2/Si interface," *J. Phys. D: Appl. Phys.* Vol. 40 (2007) p. 2886.

[18] M. Ribeiro, L. C. Fonseca, and, L.G. Ferreira, "Accurate prediction of the Si/SiO2 interface band offset using the self-consistent *ab initio* DFT/LDA-1/2 method," *Phys. Rev. B*, Vol. 79 (2009) 241312G.

[19] "Semiconductors group IV elements and III-V compounds", ed. O. Madelung, Springer, 1991

[20] P. Carrier, L. J. Lewis, and, M. W. C. Dharma-wardana, "Optical properties of structurally relaxed SiO/SiO$_2$ superlattices: The role of bonding at interfaces," *Phys. Rev. B*, Vol. 65, p.165339, 2002.

[21] E. Barbagiovanni, D. Lockwood, P. Simpson, and, L. Goncharova, "Quantum confinement in Si and Ge nanostructures," *J. Appl. Phys.*, Vol. 111, p. 034307, 2012.

[22] N. J. Ramer and A. M. Rappe, "Virtual-crystal approximation that works: locating a compositional phase boundary in Pb(Zr$_{1-x}$Ti$_x$)O$_3$,", *Phys. Rev. B*, Vol. 62, R743, 2000.